doi:10.1093/brain/awh493 *Brain* (2005), **128,** 1595–1604

Brain tissue damage in dementia with Lewy bodies: an *in vivo* diffusion tensor MRI study

M. Bozzali,[1,3] A. Falini,[2] M. Cercignani,[4] F. Baglio,[1] E. Farina,[1] M. Alberoni,[1] P. Vezzulli,[2] F. Olivotto,[1] F. Mantovani[1], T. Shallice,[3] G. Scotti,[2] N. Canal[1] and R. Nemni[1]

[1]Don Carlo Gnocchi Foundation, Scientific Institute and University, IRCCS, [2]Department of Neuroradiology, Scientific Institute and University Ospedale San Raffaele, Milan, Italy and [3]Institute of Cognitive Neuroscience and [4]NMR Research Unit, Institute of Neurology, University College London, London, UK

Correspondence to: Dr Marco Bozzali, Wellcome Department of Imaging Neuroscience, Institute of Neurology, University College London, 12 Queen Square, London WC1N 3BG, UK
E-mail: m.bozzali@fil.ion.ucl.ac.uk

The aim of the present study was to apply diffusion tensor MRI (DT-MRI), a quantitative MRI measure which reflects tissue organization, to dementia with Lewy bodies (DLB). DT-MRI scans were obtained from 15 patients with probable DLB and 10 sex- and age-matched healthy controls. Abnormalities were found in the corpus callosum, pericallosal areas and the frontal, parietal, occipital and, less prominently, temporal white matter of patients compared with controls. Abnormalities were also found in the caudate nucleus and the putamen. The average grey matter volume was lower in patients than in controls. These findings of concomitant grey matter atrophy and white matter abnormalities (as detected by DT-MRI) in regions with a high prevalence of long connecting fibre tracts might suggest the presence of neurodegeneration involving associative cortices. The modest involvement of the temporal lobe fits with the relative preservation of global neuropsychological measures and memory tasks in the early stage of DLB. The selective involvement of parietal, frontal and occipital lobes might explain some of the clinical and neuropsychological features of DLB, providing a possible distinctive marker for this disease. The abnormalities found in the subcortical grey matter may indicate that DLB and Parkinson's disease share a similar nigrostriatal involvement caused by common pathophysiological mechanisms.

Keywords: dementia; diffusion tensor; Lewy body; MRI; neuropsychological

Abbreviations: $\overline{D}$ = mean diffusivity; DLB = dementia with Lewy bodies; DT-MRI = diffusion tensor magnetic resonance imaging; DWMHs = deep white matter hyperintensitivites; EPI = echo-planar imaging; FA = fractional anisotropy; MMSE = Mini-Mental State Examination; MPRAGE = magnetization-prepared rapid-acquisition gradient echo; PGSE = pulsed gradient spin-echo; PVH = periventricular hyperintensity; ROI = region of interest; SPECT = single photon emission computed tomography; TE = echo time; TI = inversion time; TR = repetition time; TSE = turbo spin-echo; VOSP = Visual Object Space and Perception

Received October 5, 2004. Revised March 1, 2005. Accepted March 2, 2005. Advance Access publication April 7, 2005

Introduction

Several pathological studies (Hansen *et al.*, 1990; Perry *et al.*, 1990) recognized dementia with Lewy bodies (DLB) as the second most common form of dementia after Alzheimer's disease, with an estimated prevalence of 0.6% in 65-year-old or older subjects from the Western world (Jellinger, 1996; Perry *et al.*, 1990). In 1996, consensus criteria for clinical diagnosis of DLB were introduced (McKeith *et al.*, 1996). Although their application to clinical practice has generally shown high specificity, a relevant percentage (ranging from 17 to 78% of cases) of missed diagnoses is still reported (McKeith *et al.*, 1999).

The pathophysiological mechanisms underlying the clinical manifestations of DLB remain largely obscure. In pathological studies, a widespread distribution of Lewy bodies has been observed in the neocortex, limbic structures, subcortical nuclei and brainstem of patients with DLB (McKeith *et al.*, 1996; Spillantini *et al.*, 1998). The extent and distribution of such abnormalities might account for the wide spectrum of neurological and psychiatric manifestations observed in DLB (Lennox *et al.*, 1989; McKeith, 1998).

MRI represents a powerful, non-invasive technique for *in vivo* soft tissue imaging with detailed anatomical resolution.

Conventional MRI has shown high sensitivity in detecting macroscopic abnormalities occurring in several neurological conditions, such as cerebral–vascular disease, multiple sclerosis and brain tumours. In such conditions, conventional MRI can provide a substantial contribution in both diagnosis and therapy. However, conventional MRI provides only non-specific information when applied to pathological conditions such as neurodegenerative diseases, its main role remaining the exclusion of alternative possible diagnoses. So far, no specific neuroradiological features of DLB have been identified by conventional MRI studies, the main abnormalities consisting in moderate brain temporal atrophy compared with that usually found in patients with Alzheimer's disease (Hashimoto *et al.*, 1998; Barber *et al.*, 1999*a*, 2000*a*).

Diffusion-weighted MRI provides a unique form of MR contrast that enables the diffusional motion of water molecules to be measured and, as a consequence of the interactions between tissue water and cellular structures, provides information about the size, shape, orientation and geometry of brain structures (Le Bihan, 1991). Pathological processes that modify tissue integrity, including the neurodegeneration occurring in DLB, can result in an increased diffusion coefficient, which can be measured *in vivo* by using MRI. The diffusion coefficient measured in the human brain by MRI is generally dependent upon the direction along which it is measured, i.e. it is anisotropic. Such anisotropy reflects, to some extent, the underlying fibre structure. This observation prompted the development of diffusion tensor MRI (DT-MRI) (Basser *et al.*, 1994). From the tensor, it is possible to derive the mean diffusivity ($\overline{D}$ = 1/3 of the trace of the tensor) and the fractional anisotropy (FA), which is one of the most robust measures of anisotropy (Pierpaoli and Basser, 1996).

The information that can be derived from regional measurement of $\overline{D}$ and FA can provide indirect insights into the brain microstructural characteristics occurring in patients with DLB, improving our comprehension of the underlying pathophysiological processes that eventually result in brain tissue loss.

DLB presents substantial differences when comparing its clinical manifestations and cognitive impairment with those that typically characterize patients with Alzheimer's disease. The main clinical features that may suggest the diagnosis of DLB include cognitive fluctuations, hallucinations, extrapyramidal signs, and sensitivity to neuroleptic drugs. From a psychometric point of view, several studies have suggested that memory impairment is less severe in patients with DLB than in those with Alzheimer's disease, while in general there are more severe impairments in visuospatial (Hansen *et al.*, 1990; Shimomura *et al.*, 1998), attentional and executive abilities (Sahgal *et al.*, 1995). As a consequence, a different pathological involvement of brain structures is likely to occur in the two different diseases. DT-MRI could have a substantial role in differentiating *in vivo* the pathological substrates underlying the two forms of dementia, possibly improving diagnostic confidence. Previously, DT-MRI has been successfully applied to Alzheimer's disease (Rose *et al.*, 2000; Bozzali *et al.*, 2001, 2002*a*), showing characteristic abnormalities in both grey matter (Bozzali *et al.*, 2001) and white matter (Rose *et al.*, 2000; Bozzali *et al.*, 2002*a*) that are undetected on conventional MRI scans.

The aims of the present study were: (i) to assess *in vivo* the presence and extent of brain tissue abnormalities in patients with DLB using DT-MRI; (ii) to investigate the presence of potentially more specific neuroradiological markers of DLB; and (iii) to find possible associations between the distribution of tissue changes and neuropsychological measures from patients with DLB.

Patients and methods

Patients

Twenty patients diagnosed with probable DLB by consensus criteria (McKeith *et al.*, 1996) were recruited for the present study from patients attending a specialist dementia clinic. As explained below (see MRI analysis and post-processing), subjects with radiological signs of concomitant cerebral vascular effects on conventional MRI were excluded from the analysis, as recommended by the criteria for clinical diagnosis of DLB (McKeith *et al.*, 1996). In such cases, vascular pathology might be at least partially responsible for cognitive deficits, making the diagnosis of DLB less plausible. As a consequence, five patients with DLB were not considered for further analysis. The main demographic and clinical data for the remaining patients (n = 15, eight women and seven men, mean age 77.1 years, range 69–88 years; median disease duration 34.5 months, range 16–109 months) are summarized in Table 1. All the subjects included fulfilled McKeith's criteria for DLB diagnosis. Since the McKhann criteria for diagnosis of probable AD explicitly require the exclusion of any other possible cause of cognitive decline (including DLB), this implies that none of the enrolled DLB patients fulfilled either possible or probable diagnosis for Alzheimer's disease. Moreover, parkinsonism (which is an uncommon feature of AD, at least in its early stages) was present in all of them from the beginning.

Thirteen sex-and age-matched healthy volunteers were enrolled as the control group. All the control subjects had no complaints of cognitive problems and no evidence of cognitive deficits on formal testing. Major systemic, psychiatric and other neurological illnesses were carefully investigated and excluded in all the subjects studied. The same radiological criteria applied to the patient cohort were used to exclude healthy subjects with radiological signs suggestive of vascular effects (n = 3). The mean age of the remaining group (n = 10) was 75.3 years, range 69–82 years, and the female : male ratio was 6 : 4.

Local ethics committee approval and written informed consent (from the subject or from the responsible guardian if the subject was incapable) were obtained before study initiation.

Neuropsychological assessment

To obtain a complete assessment of the cognitive function in each subject studied, an extensive neuropsychological battery was administered by two trained neuropsychologists 48 h before the acquisition of the MRIs. This included the Mini-Mental State Examination (MMSE) (Folstein *et al.*, 1975; Magni *et al.*, 1996), the Token Test (Spinnler and Tognoni, 1987), forward and backward digit span test

Table 1 Demographic and principal clinical data from patients with DLB

Case	Age (years)	Sex	Diagnosis	Disease duration (months)	Clinical features*
1	69	F	Probable	16	Cog decl; Vis hall; Park; Flu cogn
2	75	M	Probable	39	Cog decl; Vis hall; Park; Flu cogn
3	79	M	Probable	22	Cog decl; Vis hall; Park; Flu cogn
4	80	F	Probable	83	Cog decl; Vis hall; Park; Flu cogn
5	75	M	Probable	34	Cog decl; Vis hall; Park; Flu cogn
6	81	M	Probable	24	Cog decl; Vis hall; Park; Flu cogn
7	88	M	Probable	35	Cog decl; Vis hall; Park; Flu cogn
8	78	F	Probable	18	Cog decl; Vis hall; Park; Flu cogn
9	76	F	Probable	26	Cog decl; Vis hall; Park; Flu cogn
10	69	F	Probable	35	Cog decl; Park; Flu cogn
11	82	F	Probable	77	Cog decl; Park; Flu cogn
12	76	M	Probable	16	Cog decl; Park; Flu cogn
13	76	F	Probable	99	Cog decl; Vis hall; Park
14	82	M	Probable	109	Cog decl; Vis hall; Park
15	70	F	Probable	106	Cog decl; Vis hall; Park

*Cog decl = progressive cognitive decline; Flu cogn = fluctuating cognition; Park = parkinsonism; Vis hall = visual hallucinations.

(Novelli *et al.*, 1986), Della Sala's dual performance test (Della Sala *et al.*, 1995), phonemic and categorical fluency tests (Novelli *et al.*, 1986), della Rocchetta's classification and recall test (della Rocchetta 1986; Pomati *et al.*, 1996), fragmented letter subtests derived from the Visual Object Space and Perception (VOSP) battery (Warrington and James, 1991), visuoperceptual tasks (Mori *et al.*, 2000) and a test for constructional praxis ability (Spinnler and Tognoni, 1987). All the scores obtained from each test were corrected for age and the level of education (conversion formulae are reported in the appropriate references), with the exception of the VOSP battery and Mori's test (for which no correction is available).

MRI acquisition

Brain MRI scans were obtained on a system operated at 1.5 T (Magnetom Vision; Siemens, Erlangen, Germany). In a single session, the following pulse sequences were obtained from all the recruited subjects without moving them from the scanner: (i) dual echo turbo spin echo (TSE) (TR = 3300 ms, TE = 16/98 ms, echo train length = 5); (ii) 3D T1-weighted turbo-flash magnetization-prepared rapid-acquisition gradient echo (MPRAGE) (TR = 9.7 ms; TE = 4 ms, TI = 300 ms, flip angle = 12°); (iii) pulsed-gradient spin-echo (PGSE) echo-planar (EPI) pulse sequence (inter-echo spacing = 0.8 ms, TE = 123 ms), with diffusion gradients applied along 8 non-collinear directions, chosen to cover 3D space uniformly (Jones *et al.*, 1999). The duration and maximum amplitude of the diffusion gradients were respectively 25 ms and 21 mT m^{-1}, giving a maximum b factor in each direction of 1044 s mm^{-2}. In order to optimize the measurement of diffusion, only two b factors were used (Bito *et al.*, 1995) ($b_1 \approx 0$, b_2 = 1044 s mm^{-2}). Fat saturation was performed using a four radiofrequency binomial pulse train to avoid chemical shift artefact. For both dual-echo and PGSE EPI sequences, 20 contiguous interleaved axial slices were acquired with 6 mm slice thickness. Dual-echo and PGSE EPI images had a 256 × 256 and 128 × 128 matrix respectively over a 250 × 250 mm field of view. The slices were positioned to run parallel to a line that joins the most inferoanterior and inferoposterior parts of the corpus callosum, covering the entire brain. The 3D-MPRAGE was acquired with sagittal orientation, with a 200 × 256 matrix and 250 × 250 mm field of view. All slice-encoding locations were acquired in a single slab, covering the whole brain, with an effective thickness of 1 mm.

MRI analysis and post-processing

Two experienced observers, unaware of to whom the scans belonged, identified by consensus any pathological T2 hyperintensities on the hard copies from patients and controls. In order to limit the risk of including subjects with concomitant vascular pathology, subjects with one or more macroscopic T2-weighted abnormalities located in the deep white matter (deep white matter hyperintensities, DWMHs) or more than five abnormalities (maximum diameter <5 mm) located in periventricular regions (periventricular hyperintensities, PVHs) were excluded from the analysis.

All images were transferred to a workstation (Sun Sparcstation; Sun Microsystems, Mountain View, CA). The 3D-MPRAGE images were processed using Matlab 6.0 (Mathwork, Natick, MA, USA) and SPM 2 (Friston *et al.*, 1995) (Wellcome Department of Cognitive Neurology, London; http://www.fil.ion.ucl.ac.uk/spm). These images were segmented into grey matter, white matter and cerebrospinal fluid using image intensity non-uniformity correction (Ashburner and Friston, 1997). In SPM, the segmentation algorithm is based on a modified model cluster analysis for grey and white matter tissue with prior knowledge of the spatial distribution of these tissues in the normal brain. In order to optimize brain extraction and tissue segmentation, these images underwent an iterative procedure (Good *et al.*, 2001). According to the optimized voxel-based morphometry approach, the extracted grey matter in native space was normalized to the grey matter template (using a combination of linear and non-linear functions), and the optimized transformation parameters were then applied to the original T1 volumes in native space. Finally, the optimally normalized images were segmented again, producing grey, white matter and cerebrospinal fluid maps in normalized space. To preserve the total within-voxel volume for grey and white matter, which may have been affected by the non-linear transformation, the signal intensity in every voxel was multiplied by the Jacobian determinants derived from the spatial normalization (Ashburner and Friston, 2000). Grey, white matter and whole-brain volume were assessed from these images for each subject.

PGSE EPI images were first corrected for geometric distortion induced by eddy currents using an algorithm which maximizes mutual information between the diffusion-unweighted and -weighted images (Studholme *et al.*, 1996). Then, assuming a mono-exponential relationship between signal intensity and the product of the b matrix and diffusion tensor matrix components, the tensor was estimated

statistically, using a multivariate linear regression model (Basser *et al.*, 1994). $\overline{D}$ and FA maps were derived (Pierpaoli and Basser, 1996).

For all subjects, anatomical regions of interest (ROIs) were selected on the b_0 step of DT-MRI scans and then transferred onto the $\overline{D}$ and FA maps in order to measure the corresponding regional quantities (Fig. 1). Rectangular ROIs of variable size (range 11.4–46.7 mm^2), depending on the anatomical region studied, were placed bilaterally in the following areas: the genu and the splenium of the corpus callosum, the posterior limb and the genu of the internal capsule, anterior and posterior pericallosal areas, the white matter of the frontal, parietal, temporal and occipital lobes, the thalamus, the putamen and the head of the caudate nucleus. The genu and the splenium of the corpus callosum were sampled on the two consecutive slices on which they were fully volumed. Anterior and posterior pericallosal ROIs were positioned laterally to the splenium and the genu of the corpus callosum in the same two slices. The posterior limb and the genu of the internal capsule, respectively indexed as the regions bounded by the corner between the head of the caudate nucleus and the pallidum and by the pallidum and the thalamus, were marked on one slice. Frontal white matter was sampled on two contiguous slices starting from the most cranial slice that included a fully volumed lateral ventricle in at least one hemisphere. Parietal lobe ROIs were positioned in the white matter posterior to the central sulcus on the most caudal slice where it was visible and on the subsequent more cranial slice. Temporal white matter was sampled on two contiguous slices and the ROIs were placed posterolaterally to the lateral fissure, starting from the most caudal slice on which it was present. The occipital white matter ROIs were placed within the optic radiations on two contiguous slices, starting from the most caudal slice on which the occipital horn of the lateral ventricle was imaged. Finally, the thalamus, the putamen and the head of the caudate nucleus were sampled by placing the ROIs in the centre of each structure, selecting the slice where each of them was more clearly detectable. Figure 1 illustrates the location of all the selected ROIs. The ROIs were transferred onto $\overline{D}$ and FA maps for each subject, and average $\overline{D}$ and FA were calculated for every ROI.

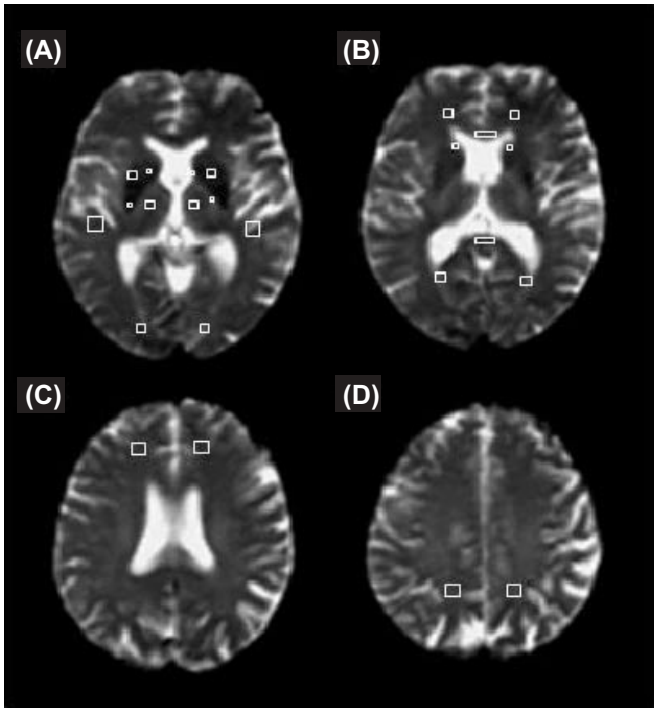

Fig. 1 Location of the selected regions of interest (ROIs) in a patient with DLB. (**A**) Internal capsule, putamen, thalamus, temporal and occipital lobes. (**B**) Genu and splenium of the corpus callosum, anterior and posterior pericallosal areas and caudate nucleus. (**C**) Frontal lobes. (**D**) Parietal lobes. See text for further details.

Statistical analysis

Student's *t*-test for non-paired data was used to compare whole brain, grey and white matter volumes, and $\overline{D}$ and FA values of the ROIs measured from patients with DLB and controls. To correct for multiple comparisons and to minimize the risk of type II errors, only *P* values $\leq$0.005 were considered statistically significant. The correlations between grey matter volumes, disease duration and a selection of neuropsychological measures were investigated in the patient group using the Spearman rank correlation coefficient. To account for the possible association between FA and $\overline{D}$, the relationship between a subset of neuropsychological tests and these two variables was assessed using linear regression with backward elimination. The model included a constant and the mean $\overline{D}$ and FA of given ROIs, decided *a priori* according to the functions assessed by a specific test. To reduce the number of comparisons, the following neuropsychological tests only were included in the analysis: MMSE (Folstein *et al.*, 1975; Magni *et al.*, 1996), as a global measure of cognitive impairment, Della Sala's dual performance test (Della Sala *et al.*, 1995), phonemic and categorical fluency tests, as measures of executive functions, the fragmented letter subtest derived from the VOSP battery (Warrington and James, 1991), shape and form discrimination from Mori's test (Mori *et al.*, 2000), as measures of visual perceptual functions, and a test for constructional praxis ability (Spinnler and Tognoni, 1987). The MMSE was regressed against the mean FA and $\overline{D}$ from frontal, parietal, temporal and occipital white matter; executive tests (dual performance, phonemic and categorical fluency tests) were regressed against the mean FA and $\overline{D}$ from frontal white matter only; the scores from the fragmented letter subtest derived from the VOSP battery were regressed against the mean FA and $\overline{D}$ from occipital, parietal and temporal white matter; Mori's test scores were regressed against the mean FA and $\overline{D}$ from parietal and occipital white matter; the scores from tests for constructional praxis ability were regressed against mean FA and $\overline{D}$ from parietal white matter.

In order to interpret the coefficients of linear regressions, one should consider that neurodegenerative processes are likely to result in a less restricted molecular mobility, and therefore in an increased $\overline{D}$ and a reduced FA. As a consequence, if an association exists between the scores in any neuropsychological test and DTI-derived measures, worse performances are expected to be related to higher $\overline{D}$ and lower FA values.

Results

Neuropsychological assessments

All the healthy subjects showed normal scores in all tests administered, with a median MMSE score (corrected for age and the level of education) of 28.6 (range 26.8–30.0). The patients with DLB reported a median MMSE score (corrected for age and the level of education) of 22.7 (range 9.3–26.7).

Table 2 Mean (SD) brain volumes (ml) of DLB patients and controls

	Controls	Patients with DLB	*P**
WB volume	1015 (102)	954 (82)	NS (0.09)
GM volume	582 (63)	518 (40)	**0.003**
WM volume	434 (47)	437 (50)	NS (0.88)

Volumes of the whole brain and segmented white and grey matter from patients with DLB and controls. *Student's *t*-test for non-paired data. WB = whole brain; GM = grey matter; WM = white matter; NS = not significant. Significant *P* values are highlighted in bold type.

In the patient group, remarkable deficits in visuospatial abilities (with low scores in 73.3% of cases in the fragmented letter subtest derived from the VOSP battery and in 60% by Mori's size discrimination test) and in working memory (with low scores in 73.3% of cases in both digit span backwards and phonemic fluency tests) were found. Relative preservation of short-term memory for verbal items was found (digit span forward scores were within the normal range in 86.6% and borderline in 13.3% of the patients studied). Finally, low scores were achieved by 20% of the cases in della Rocchetta's recall test, and by 26.6% of the cases in the test for constructional praxis ability of Spinnler and Tognoni.

Conventional MRI and brain volumes

Non-specific white matter PVHs were detected on scans from five controls and six patients with DLB. However, the number of lesions was not statistically different between patients and controls [mean (SD) number was 2.7 (1.2) and 2.5 (1.3) respectively; $P = 0.89$]. By definition, there were no more than five lesions per subject and the lesions were <5 mm in diameter.

Grey, white matter and whole-brain volumes are reported in Table 2. The average whole-brain volume was reduced in DLB patients compared with controls, although the difference did not reach statistical significance ($P = 0.09$). No significant difference was found comparing white matter volumes between the two groups ($P = 0.88$). Conversely, a significant volume reduction was found in patients compared with controls when considering grey matter in isolation ($P = 0.003$).

Diffusion tensor imaging

The selected ROIs and the corresponding mean $\overline{D}$ and FA average values from patients and controls are reported in Tables 3 and 4. In two cases (one patient and one control), a previously identified area of PVH was located in the proximity of a pericallosal ROI. $\overline{D}$ and FA values from these two ROIs were excluded from the statistical analysis. Areas of significant increases of $\overline{D}$ were found in the frontal, parietal and occipital white matter, in the corpus callosum and pericallosal areas, and in the caudate nucleus of DLB patient compared with controls. Areas of significant decreases of FA were found in the frontal, parietal, occipital and temporal white matter, in the corpus callosum and in the pericallosal regions of DLB patients compared with controls. A trend towards statistical significant difference was found for both mean $\overline{D}$ and FA of the putamen between patients and controls, with higher $\overline{D}$ and lower FA values in the former group of subjects.

Table 3 Mean (SD) $\overline{D}$ values of the selected areas from DLB patients and controls

	Controls	Patients with DLB	*P**
Frontal white matter	0.80 (0.05)	0.94 (0.06)	<**0.001**
Parietal white matter	0.82 (0.04)	1.00 (0.09)	<**0.001**
Temporal white matter	0.87 (0.05)	0.91 (0.05)	NS (0.40)
Occipital white matter	0.90 (0.08)	1.00 (0.10)	**0.001**
Corpus callosum	0.85 (0.06)	1.02 (0.13)	<**0.001**
Pericallosal areas	0.84 (0.04)	0.96 (0.09)	<**0.001**
Internal capsule	0.81 (0.04)	0.82 (0.04)	NS (0.42)
Thalamus	0.84 (0.02)	0.88 (0.08)	NS (0.15)
Caudate nucleus	0.76 (0.07)	0.91 (0.08)	<**0.001**
Putamen	0.85 (0.06)	0.94 (0.10)	NS (0.007)

Corpus callosum $\overline{D}$ values were obtained by averaging the values of the splenium and genu of the corpus callosum. Pericallosal $\overline{D}$ values were obtained by averaging the values of the anterior and posterior pericallosal areas. Internal capsule $\overline{D}$ values were obtained by averaging the values of genu and posterior limb of this structure. See text for further details. *Student's *t*-test for non-paired data (only Bonferroni-corrected *P* values ≤ 0.005 were considered statistically significant); $\overline{D}$ = mean diffusivity, expressed in units of $mm^2\ s^{-1} \times 10^{-3}$; NS = not significant. Significant *P* values are highlighted in bold type.

Table 4 Mean (SD) FA values of the selected areas from DLB patients and controls

	Controls	Patients with DLB	*P**
Frontal white matter	0.32 (0.03)	0.26 (0.03)	<**0.001**
Parietal white matter	0.34 (0.03)	0.27 (0.03)	<**0.001**
Temporal white matter	0.25 (0.02)	0.21 (0.02)	<**0.001**
Occipital white matter	0.22 (0.04)	0.16 (0.03)	<**0.001**
Corpus callosum	0.66 (0.08)	0.51 (0.06)	<**0.001**
Pericallosal areas	0.37 (0.04)	0.30 (0.04)	<**0.001**
Internal capsule	0.45 (0.06)	0.45 (0.04)	NS (0.91)
Thalamus	0.31 (0.06)	0.31 (0.07)	NS (0.83)
Caudate nucleus	0.26 (0.06)	0.21 (0.06)	NS (0.06)
Putamen	0.25 (0.05)	0.20 (0.03)	NS (0.008)

Pericallosal FA values were obtained by averaging the values of the anterior and posterior pericallosal areas. Internal capsule FA values were obtained by averaging the values of the genu and posterior limb of this structure. See text for further details. Corpus callosum FA values were obtained by averaging the values of the splenium and genu of the corpus callosum. *Student's *t*-test for non-paired data (only Bonferroni-corrected *P* values ≤ 0.005 were considered statistically significant). FA = fractional anisotropy; NS = not significant. Significant *P* values are highlighted in bold type.

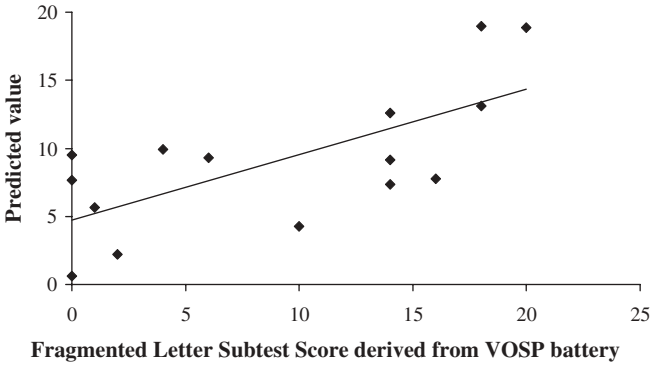

Fig. 2 Scatter plot of scores obtained from the fragmented letter subset score derived from the Visual Object Space and Perception (VOSP) battery versus their values predicted by a linear regression model based on DT-MRI metrics measured in the temporal white matter (WM) of patients with DLB. Three predictors [mean diffusivity ($\overline{D}$), fractional anisotropy (FA) and a constant] were entered in the model, giving $r = 0.8$, $P = 0.008$. See text for further details.

Associations between MRI-derived metrics and disease duration and neuropsychological measures in the patient group

Grey matter volume was found to correlate inversely with disease duration ($r = -0.74$, $P = 0.002$). No association was found between MMSE score and any of the MRI-derived metrics considered. The best predicting model for Della Sala's dual performance test ($r = 0.60$, $P = 0.01$) included a constant (326.7, $P = 0.002$) and $\overline{D}$ of frontal white matter (coefficient = −255, $P = 0.01$). The best predicting model for the phonemic fluency test ($r = 0.55$, $P = 0.03$) included a constant (–18.1, $P = 0.2$) and FA of frontal white matter (coefficient = 92.2, $P = 0.03$). The best predicting model for the categorical fluency test ($r = 0.69$, $P = 0.004$) included a constant (–33.7, $P = 0.02$) and FA of frontal white matter (coefficient = 167, $P = 0.004$). The best predicting model for the fragmented letter subtest derived from the VOSP battery ($r = 0.80$, $P = 0.008$) included a constant (32.1, $P = 0.36$), $\overline{D}$ (coefficient = −68.5, $P = 0.04$) and FA (coefficient = 265, $P = 0.008$) of temporal white matter (Fig. 2). The best predicting model for the size discrimination from Mori's test ($r = 0.70$, $P = 0.03$) included a constant (30.6, $P < 0.001$), $\overline{D}$ of parietal white matter (coefficient = −6.4, $P = 0.06$) and $\overline{D}$ of occipital white matter (coefficient = −5.3, $P = 0.07$). The best predicting model for the shape discrimination from Mori's test ($r = 0.80$, $P < 0.001$) included a constant (–26.3, $P = 0.01$) and FA of parietal white matter (coefficient = 146, $P < 0.001$). The best predicting model for the constructional praxis ability test ($r = 0.65$, $P = 0.008$) included a constant (–19.8, $P = 0.05$) and FA of parietal white matter (coefficient = 105, $P = 0.008$).

Discussion

To our knowledge this is the first application of DT-MRI to a group of patients with DLB. DT-MRI represents a unique technique in terms of providing *in vivo* indirect information on the cellular tissue structure and damage. This quantitative approach has already been applied successfully to several neurological (Lutsep *et al.*, 1997; Chabriat *et al.*, 1999; Werring *et al.*, 1999; Rose *et al.*, 2000; Bozzali *et al.*, 2001, 2002*a*, *b*; Gauvain *et al.*, 2001; Eriksson *et al.*, 2001) and psychiatric (Lim *et al.*, 1999; Alexopoulos *et al.*, 2002; Burns *et al.*, 2003) diseases, showing its potential to provide insights into their underlying pathophysiological mechanisms. In a previous study, using a similar approach, Bozzali and colleagues studied a group of patients with Alzheimer's disease, finding characteristic abnormalities and strong correlations between global neuropsychological measures and DT-MRI derived quantities (Bozzali *et al.*, 2002*a*).

The neuropsychological assessment of the patients recruited in the present study revealed, as expected, the typical profile of DLB, characterized by relatively modest global impairment and prominent deficits in visuospatial abilities and in working memory (backward span), with relative preservation of short-term storage *per se* (forward span). As a consequence of the exclusion criteria, the presence of macroscopic T2-weighted abnormalities was very modest both in patients with DLB and in controls, thus increasing our confidence that the enrolled patients presented with a relatively pure degenerative form and that there was hardly any contribution from concomitant cerebral vascular disease, as recommended by consensus criteria for the diagnosis of DLB (McKeith *et al.*, 1996). Non-specific PVHs similar to those we found in this study have been described previously in both healthy elderly subjects (Meyer *et al.*, 1992) and patients with dementia (Mirsen and Merskey *et al.*, 1994; Fazekas *et al.*, 1996; O'Brien *et al.*, 1996). Such abnormalities are believed to be associated with the normal ageing processes in healthy subjects (Meyer *et al.*, 1992) and to be more severe when late-onset degenerative dementias occur (Barber *et al.*, 1999b). Although their aetiology and pathology are still inadequately understood, PVHs have been suggested to be an epiphenomenon of brain atrophy (Fazekas *et al.*, 1996; Barber *et al.*, 2000*b*). Conversely, in a study on patients with Alzheimer's disease, DWMHs have been found to correlate with vascular risk factors (Brun *et al.*, 1986), suggesting a distinct aetiology.

Although the average whole-brain volume was lower in patients with DLB than in controls, suggesting the presence of moderate widespread atrophy, such a difference did not reach statistical significance. This result is consistent with previous reports (Barber *et al.*, 1999*a*, 2000*a*), indicating less prominent brain volume loss in patients with DLB than in those with Alzheimer's disease. Nevertheless, the volumetric analysis after image segmentation, showed a significant reduction of grey matter volume in patients with DLB compared with controls, without any significant difference

in white matter volume. Grey matter volume was also found to be inversely correlated with disease duration. These findings suggest that the tissue damage occurring in DLB could at least partially reflect some involvement of neurons located in the association cortex, possibly related to the progression of the disease.

An attempt to localize the main areas of grey matter tissue damage was made by Burton and colleagues, who studied a group of patients with DLB using voxel-based morphometry (Burton *et al.*, 2002). However, such a technique can identify only macroscopic tissue loss affecting grey matter in isolation, which might represent just the ultimate result of the microscopic underlying pathology. By contrast, DT-MRI is sensitive to changes undetected by conventional MRI, and DT-MRI-derived quantities can reflect to some extent tissue structural abnormalities at the subvoxel level. In this study, we found concomitant increased $\overline{D}$ and decreased FA values in the corpus callosum and pericallosal areas of patients with DLB compared with controls. When considered in association with grey matter atrophy, the location of white matter structural abnormalities in these regions with a high prevalence of fibre tracts connecting cortical associative areas suggests the presence of some pathophysiological processes that eventually affect neurons in the association cortex. However, the nature of the tissue damage occurring in DLB is still unclear, particularly due to the lack of post-mortem evidence of Wallerian degeneration (Katsuse *et al.*, 2003) and demyelination (Higuchi *et al.*, 2000). A proton MR spectroscopy study on patients in the early stages of DLB reported abnormalities involving white matter in the absence of any grey matter change (Molina *et al.*, 2002), and a neuropathological study suggested that the presence of widespread spongiform changes and gliosis affecting long projection fibres contributes to DLB pathophysiology (Higuchi *et al.*, 2000). DT-MRI provides information about the diffusional motion of water as a result of the interactions between tissue water and cellular structures. Pathological processes that modify cell microstructure, such as changes involving the neuronal distribution of cytoskeletal elements, might therefore result in $\overline{D}$ or FA changes. Shepherd and colleagues described a significant increase in the number of neurons immunoreactive for the non-phosphorylated 200-kDa neurofilament (NF) in the frontal and temporal cortex of DLB patients compared with Alzheimer's disease patients (Shepherd *et al.*, 2002). NF proteins are supposed to play an important role in maintaining axon calibre. Moreover, axonal transport blockage has been found to be associated with the formation of Lewy bodies (Katsuse *et al.*, 2003). Such findings could contribute to an explanation of neuronal dysfunction in the absence of marked brain atrophy, and of the diffusion abnormalities found in the present study.

Any attempt to interpret the substrate of the changes found in DT-MRI derived quantities is purely speculative, as their origin could only be confirmed by a post-mortem examination; however, we would like to focus our attention on the anatomical location of such abnormalities as this might help in understanding some of the clinical features of the disease. Although the pathophysiological mechanisms and the underlying pathological tissue damage in DLB and Alzheimer's disease are likely to be different, similar DT-MRI results had been found in a previous study on patients with Alzheimer's disease (Bozzali *et al.*, 2002*a*), revealing marked involvement of the corpus callosum and pericallosal areas. These white matter abnormalities might contribute to the neuropsychological impairment in both patients with Alzheimer's disease and patients with DLB. Although the lack of a group of patients with Alzheimer's disease in this study prevents a direct evaluation, one could speculate on the different topographic pattern of structural white matter abnormalities revealed by this study on DLB compared with previous studies on Alzheimer's disease (Bozzali *et al.*, 2001, 2002*a*). Within the limitations of an indirect comparison, it is interesting to note that in patients with Alzheimer's disease compared with controls, $\overline{D}$ was found to be significantly increased in the white matter of the temporal and parietal lobes with a concomitant decrease in FA in the same regions and an isolated decrease in FA in the frontal lobe white matter. Similar $\overline{D}$ and FA quantities were found when comparing the values obtained from occipital white matter between patients with Alzheimer's disease and controls (Bozzali *et al.*, 2002*a*). In the present study, patients with DLB showed less prominent involvement of temporal white matter, with significantly decreased FA but no significant difference in $\overline{D}$ values. Consistently, memory deficits can be modest, at least in the early stages of the disease (McKeith *et al.*, 1996) and previous MRI studies have shown relative preservation of medial temporal lobe volume in DLB compared with Alzheimer's disease patients (Barber *et al.*, 1999*a*, 2000*a*). The FA abnormalities we detected in the temporal white matter of DLB patients could therefore reflect the presence of only subtle tissue damage. On the other hand, significant changes in both $\overline{D}$ and FA were observed in the frontal, parietal and occipital white matter of DLB patients compared with controls. These abnormalities could account for the characteristic cognitive impairment observed in DLB. Patients with DLB typically present with substantial visuospatial and attentional deficits (Hansen *et al.*, 1990; Shimomura *et al.*, 1998) and executive dysfunction (Sahgal *et al.*, 1995). Therefore, frontal, parietal and occipital lobe white matter involvement is likely to play an important role in producing the cognitive deficits observed in DLB. In keeping with this perspective, we found in this group of patients associations between DT-MRI derived measures in the frontal lobe and categorical fluency score (a test which stresses prefrontal functions), between DT-MRI derived measures of the parietal lobe and scores from constructional praxis, well known to have parietal components (McCarthy and Warrington, 1992), and Mori's test (shape and form discrimination). Although the relatively large number of correlations we investigated increases the risk of false positives, all r values were greater than 0.5, suggesting that these results are not merely the outcome of a large number of comparisons. If confirmed by further investigations, these findings suggest a

potential role for DT-MRI in monitoring the evolution of DLB in both clinical and pharmacological trials.

Two issues deserve particular attention in terms of providing a pathophysiological interpretation of some clinical characteristics of DLB: the visuoperceptual deficits and the visual hallucinations, the latter representing one of the cardinal clinical features for the diagnosis of DLB (McKeith *et al.*, 1996). The abnormalities observed in the occipital white matter of patients fit well with the low score obtained in the fragmented letter subtest derived from VOSP, providing a possible pathophysiological explanation for the visuoperceptual deficits observed in DLB. This selective involvement of the occipital lobe, which was completely absent in a group of patients with Alzheimer's disease (Bozzali *et al.*, 2002*a*), is also consistent with previous SPECT studies (Ishii *et al.*, 1999; Higuchi *et al.*, 2000; Lobotesis *et al.*, 2001; Minoshima *et al.*, 2001; Okamura *et al.*, 2001), suggesting a possible distinctive marker for DLB (Okamura *et al.*, 2001). On the other hand, such abnormalities could also partially be responsible for the visual hallucinations that are frequently observed after occipital lobe disease (Gloning *et al.*, 1967), although a recent structural MRI study failed to demonstrate any macroscopic volume difference from the occipital lobe of patients with DLB compared with healthy controls, Alzheimer's disease and vascular patients (Middelkoop *et al.*, 2001). In our sample, 12 out of 15 (80%) patients suffered from visual hallucinations (Table 1), which fits well with the abnormal derived metrics measured in the occipital white matter of our cohort of patients.

Moreover, associations were also found among the score obtained in the fragmented letter subtest derived from VOSP battery and DT-MRI derived metrics from the temporal white matter of patients with DLB (Fig. 2). The pathogenesis of the well-formed visual hallucinations in patients with DLB is still poorly understood and possibly more than one mechanism might be involved. It is also uncertain whether visuospatial deficits and visual hallucinations have a common pathophysiological mechanism in DLB. In a recent report, Barnes and colleagues found that hallucinating patients with Parkinson's disease were particularly impaired on tests of face recognition and silhouette identification (using the VOSP battery) when compared with Parkinson's disease patients not suffering from hallucinations (Barnes *et al.*, 2003). Visuoperceptual deficits and positive phenomena of hallucinations might therefore be related to each other. Speculating on this hypothesis, the linear relationship we found between the score obtained in the fragmented letter subtest derived from the VOSP battery and temporal white matter DT-MRI-derived measures in our patient sample could then fit with the finding of a strong correlation between Lewy bodies in the temporal lobe and visual hallucinations in DLB patients that was described in a recent pathological study (Harding *et al.*, 2002). Studies on larger populations of patients with DLB are needed in order to clarify the value of such observations.

Interestingly, we also found statistically significant $\overline{D}$ changes in the caudate nucleus. The increased $\overline{D}$ with a concomitant absence of FA reduction in the caudate nucleus is not surprising, since FA is significantly lower in grey than in white matter, and therefore its measurement is largely affected by noise in grey matter areas (Pierpaoli and Basser; 1996). Abnormalities of the caudate nucleus are consistent with a previous PET study which showed a decrease in fluoro-dopa accumulation in the same structure (Hisanaga *et al.*, 2001). These findings suggest the presence of subcortical involvement in DLB, which should be further investigated in a larger study. A recent study on patients with parkinsonism and either early- (DLB) or late (Parkinson's disease plus dementia)-developing dementia revealed a marked overlap of the pathological features between the two groups (Jellinger, 2003). Therefore it would be of interest to make a direct comparison between DT-MRI-derived metrics obtained from the basal ganglia of patients with DLB and those obtained from patients with Parkinson's disease.

The main limitation of this study is the inclusion of a relatively small number of subjects. Secondly, the absence of a group of patients with Alzheimer's disease limits the interpretation of the widespread changes observed in the group of patients with DLB. A direct comparison between DT-MRI-derived metrics of patients with either pathology would strengthen the conclusions obtained from the present study and it is therefore strongly warranted. The results we obtained have to be considered as preliminary to future studies on larger samples of patients. However, the present study has shown the potential contribution of DT-MRI to the comprehension of the pathophysiological mechanisms underlying DLB. Moreover, DT-MRI might represent a powerful tool in monitoring clinical trials on drugs potentially able to affect disease evolution in patients with DLB. Finally, the different pattern of brain tissue abnormalities between patients with DLB and those with Alzheimer's disease suggested by the comparison between the results of the present study and previous ones and its consistency with previous SPECT and PET studies supports the potential usefulness of DT-MRI in providing some specific neuroradiological markers for DLB, which might improve the diagnostic criteria in clinical practice.

References

Alexopoulos GS, Kiosses DN, Choi SJ, Murphy CF, Lim KO. Frontal white matter microstructure and treatment response of late-life depression: a preliminary study. Am J Psychiatry 2002; 159: 1929–32.

Ashburner J, Friston KJ. Multimodal image coregistration and partitioning. A unified framework. Neuroimage 1997; 6: 209–17.

Ashburner J, Friston KJ. Voxel-based morphometry—the methods. Neuroimage 2000; 11: 805–21.

Barber R, Gholkar A, Scheltens P, Ballard C, McKeith IG, O'Brien JT. Medial temporal lobe atrophy on MRI in dementia with Lewy bodies. Neurology 1999a; 52: 1153–8.

Barber R, Scheltens P, Gholkar A, Ballard C, McKeith I, Ince P, et al. White matter lesions on magnetic resonance imaging in dementia with Lewy

bodies, Alzheimer's disease, vascular dementia, and normal aging. J Neurol Neurosurg Psychiatry 1999b; 67: 66–72.

Barber R, Ballard C, McKeith IG, Gholkar A, O'Brien JT. MRI volumetric study of dementia with Lewy bodies: a comparison with AD and vascular dementia. Neurology 2000a; 54: 1304–9.

Barber R, Gholkar A, Scheltens P, Ballard C, McKeith IG, O'Brien JT. MRI volumetric correlates of white matter lesions in dementia with Lewy bodies and Alzheimer's disease. Int J Geriatr Psychiatry 2000b; 15: 911–6.

Barnes J, Boubert L, Harris J, Lee A, David AS. Realty monitoring and visual hallucinations in Parkinson's disease. Neuropsychologia 2003; 41: 565–74.

Basser PJ, Mattiello J, LeBihan D. MR diffusion tensor spectroscopy and imaging. Biophys J 1994; 66: 259–67.

Bito Y, Hirata S, Yamamoto E. Optimal gradient factors for ADC measurements [abstract]. Proc Int Soc Mag Reson Med 1995; 2: 913.

Bozzali M, Franceschi M, Falini A, Pontesilli S, Cercignani M, Magnani G, et al. Quantification of tissue damage in AD using diffusion tensor and magnetization transfer MRI. Neurology 2001; 57: 1135–7.

Bozzali M, Falini A, Franceschi M, Cercignani M, Zuffi M, Scotti G, et al. White matter damage in Alzheimer's disease assessed in vivo using diffusion tensor magnetic resonance imaging. J Neurol Neurosurg Psychiatry 2002a; 72: 742–6.

Bozzali M, Cercignani M, Sormani MP, Comi G, Filippi M. Quantification of brain gray matter damage in different MS phenotypes by use of diffusion tensor MR imaging. AJNR Am J Neuroradiol 2002b; 23: 985–8.

Brun A, Englund E. A white matter disorder in dementia of the Alzheimer type: a pathoanatomical study. Ann Neurol 1986; 19: 253–62.

Burns J, Job D, Bastin ME, Whalley H, Macgillivray T, Johnstone EC, et al. Structural disconnectivity in schizophrenia: a diffusion tensor magnetic resonance imaging study. Br J Psychiatry 2003; 182: 439–43.

Burton EJ, Karas G, Paling SM, Barber R, Williams ED, Ballard CG, et al. Patterns of cerebral atrophy in dementia with Lewy bodies using voxel-based morphometry. Neuroimage 2002; 17: 618–30.

Chabriat H, Pappata S, Poupon C, Clark CA, Vahedi K, Poupon F, et al. Clinical severity in CADASIL related to ultrastructural damage in white matter: *in vivo* study with diffusion tensor MRI. Stroke 1999; 30: 2637–43.

della Rocchetta AI. Classification and recall of pictures after unilateral frontal or temporal lobectomy. Cortex 1986; 22: 189–211.

Della Sala S, Baddeley A, Papagno C, Spinnler H. Dual-task paradigm: a means to examine the central executive. Ann N Y Acad Sci 1995; 769: 161–71.

Eriksson SH, Rugg-Gunn FJ, Symms MR, Barker GJ, Duncan JS. Diffusion tensor imaging in patients with epilepsy and malformations of cortical development. Brain 2001; 124: 617–26.

Fazekas F, Kapeller P, Schmidt R, Offenbacher H, Payer F, Fazekas G. The relation of cerebral Magnetic resonance signal hyperintensites to Alzheimer's disease. J Neurol Sci 1996; 142: 121–5.

Folstein MF, Folstein SE, McHugh PR. 'Mini-mental state'. A practical method for grading the cognitive state of patients for the clinician. J Psychiatr Res 1975; 12: 189–98.

Friston KJ, Holmes AP, Worsley KJ, Poline JP, Frith CD, Frackowiak RSJ. Statistical parametric maps in functional imaging: a general linear approach. Hum Brain Mapp 1995; 2: 189–210.

Gauvain KM, McKinstry RC, Mukherjee P, Perry A, Neil JJ, Kaufman BA, et al. Evaluating pediatric brain tumor cellularity with diffusion-tensor imaging. AJR Am J Roentgenol 2001; 177: 449–54.

Gloning I, Gloning K, Hoff H. On optic hallucinations. A study based on 241 patients with lesions of the occipital lobe and its surrounding regions verified by autopsy or surgery. Wien Z Nervenheilkd Grenzgeb 1967; 25: 1–19.

Good CD, Johnsrude IS, Ashburner J, Henson RN, Friston KJ, Frackowiak RS. A voxel-based morphometric study of aging in 465 normal adult human brains. Neuroimage 2001; 14: 21–36.

Hansen L, Salmon D, Galasko D, Masliah E, Katzman R, DeTeresa R, et al. The Lewy body variant of Alzheimer's disease: a clinical and pathologic entity. Neurology 1990; 40: 1–8.

Harding AJ, Broe GA, Halliday GM. Visual hallucinations in Lewy body disease relate to Lewy bodies in the temporal lobe. Brain 2002; 125: 391–403.

Hashimoto M, Kitagaki H, Imamura T, Hirono N, Shimomura T, Kazui H, et al. Medial temporal and whole-brain atrophy in dementia with Lewy bodies: a volumetric MRI study. Neurology 1998; 51: 357–62.

Higuchi M, Tashiro M, Arai H, Okamura N, Hara S, Higuchi S, et al. Glucose hypometabolism and neuropathological correlates in brains of dementia with Lewy bodies. Exp Neurol 2000; 162: 247–56.

Hisanaga K, Suzuki H, Tanji H, Mochizuki H, Iwasaki Y, Sato N, et al. Fluoro-DOPA and FDG positron emission tomography in a case of pathological verified pure diffuse Lewy body disease. J Neurol 2001; 248: 905–6.

Ishii K, Yamaji S, Kitagaki H, Imamura T, Hirono N, Mori E. Regional cerebral blood flow difference between dementia with Lewy bodies and AD. Neurology 1999; 53: 413–7.

Jellinger KA. Structural basis of dementia in neurodegenerative disorders. J Neural Transm 1996; 47 Suppl: 1–29.

Jellinger KA. Neuropathological spectrum of synucleinopathies. Mov Disord 2003; 18 Suppl 6: S2–12.

Jones DK, Horsfield MA, Simmons A. Optimal strategies for measuring diffusion in anisotropic systems by magnetic resonance imaging. Magn Reson Med 1999; 42: 515–25.

Katsuse O, Iseki E, Marui W, Kosaka K. Developmental stages of cortical Lewy bodies and their relation to axonal transport blockage in brains of patients with dementia with Lewy bodies. J Neurol Sci 2003; 211: 29–35.

Le Bihan D. Molecular diffusion nuclear magnetic resonance imaging. Magn Reson Q 1991; 7: 1–30.

Lennox G, Lowe JS, Godwin-Austen RB, Landon M, Mayer RJ. Diffuse Lewy body disease: an important differential diagnosis in dementia with extrapyramidal features. Prog Clin Biol Res 1989; 317: 121–30.

Lim KO, Hedehus M, Moseley M, de Crespigny A, Sullivan EV, Pfefferbaum A. Compromised white matter tract integrity in schizophrenia inferred from diffusion tensor imaging. Arch Gen Psychiatry 1999; 56: 367–74.

Lobotesis K, Fenwick JD, Phipps A, Ryman A, Swann A, Ballard C, et al. Occipital hypoperfusion on SPECT in dementia with Lewy bodies but not AD. Neurology 2001; 56: 643–9.

Lutsep HL, Albers GW, De Crespigny A, Kamat GN, Marks MP, Moseley ME. Clinical utility of diffusion-weighted magnetic resonance imaging in the assessment of ischemic stroke. Ann Neurol 1997; 41: 574–80.

Magni E, Binetti G, Bianchetti A, Rozzini R, Trabucchi M. Mini-Mental State Examination: a normative study in Italian elderly population. Eur J Neurol 1996; 3: 1–5.

McCarthy RA, Warrington EK. Actors but not scripts: the dissociation of people and events in retrograde amnesia. Neuropsychologia 1992; 30: 633–44.

McKeith IG. Dementia with Lewy bodies: clinical and pathological diagnosis. Alzheimers Rep 1998; 1: 83–7.

McKeith IG, Galasko D, Kosaka K, Perry EK, Dickson DW, Hansen LA, et al. Consensus guidelines for the clinical and pathologic diagnosis of dementia with Lewy bodies (DLB): report of the consortium on DLB international workshop. Neurology 1996; 47: 1113–24.

McKeith IG, O'Brien JT, Ballard C. Diagnosing dementia with Lewy bodies. Lancet 1999; 354: 1227–8.

McKhann G, Drachman D, Folstein M, Katzman R, Price D, Stadlan EM. Clinical diagnosis of Alzheimer's disease: report of the NINCDS- ADRDA work Group under the auspices of Department of Health and Human Services Task force on Alzheimer's Disease. Neurology 1984; 34: 939–44.

Meyer JS, Kawamura J, Terayama Y. White matter lesions in the elderly. J Neurol Sci 1992; 110: 1–7.

Middelkoop HA, van der Flier WM, Burton EJ, Lloyd AJ, Paling S, Barber R, et al. Dementia with Lewy bodies and AD are not associated with occipital lobe atrophy on MRI. Neurology 2001; 57: 2117–20.

Minoshima S, Foster NL, Sima AA, Frey KA, Albin RL, Kuhl DE. Alzheimer's disease versus dementia with Lewy bodies: cerebral

metabolic distinction with autopsy confirmation. Ann Neurol 2001; 50: 358–65.

Mirsen TR, Merskey H. Leukoaraiosis. In: Burns A, Lewy R, editors. Dementia. London: Chapman and Hall; 1994. p. 641–52.

Molina JA, Garcia-Segura JM, Benito-Leon J, Gomez-Escalonilla C, del Ser T, Martinez V, et al. Proton magnetic resonance spectroscopy in dementia with Lewy bodies. Eur Neurol 2002; 48: 158–63.

Mori E, Shimomura T, Fujimori M, Hirono N, Imamura T, Hashimoto M, et al. Visuoperceptual impairment in dementia with Lewy bodies. Arch Neurol 2000; 57: 489–93.

Novelli G, Pagano C, Capitani E. Tre test di ricerca e produzione lessicale. Archiv Psicol Neurol Psichiatr 1986; 47: 477–506.

O'Brien JT, Ames D, Schweitzer I. White matter lesions in depression and Alzheimer's disease: a review of magnetic resonance imaging studies. Int J Geriatr Psychiatry 1996; 11: 681–94.

Okamura N, Arai H, Higuchi M, Tashiro M, Matsui T, Hu XS, et al. [18F]FDG-PET study in dementia with Lewy bodies and Alzheimer's disease. Prog Neuropsychopharmacol Biol Psychiatry 2001; 25: 447–56.

Perry RH, Irving D, Blessed G, Fairbairn A, Perry EK. Senile dementia of Lewy body type. A clinically and neuropathologically distinct form of Lewy body dementia in the elderly. J Neurol Sci 1990; 95: 119–39.

Pierpaoli C, Basser PJ. Toward a quantitative assessment of diffusion anisotropy. Magn Reson Med 1996; 36: 893–906.

Pomati S, Farina E, Magni E, Laiacona M, Mariani C. Normative data for two neuropsychological tests sensitive to frontal dysfunction. Ital J Neurol Sci 1996; 17: 201–9.

Rose SE, Chen F, Chalk JB, Zelaya FO, Strugnell WE, Benson M, et al. Loss of connectivity in Alzheimer's disease: an evaluation of white matter tract integrity with colour coded MR diffusion tensor imaging. J Neurol Neurosurg Psychiatry 2000; 69: 528–30.

Sahgal A, McKeith IG, Galloway PH, Tasker N, Steckler T. Do differences in visuospatial ability between senile dementias of the Alzheimer and Lewy body types reflect differences solely in mnemonic function? J Clin Exp Neuropsychol 1995; 17: 35–43.

Shepherd CE, McCann H, Thiel E, Halliday GM. Neurofilament-immunoreactive neurons in Alzheimer's disease and dementia with Lewy bodies. Neurobiol Dis 2002; 9: 249–57.

Shimomura T, Mori E, Yamashita H, Imamura T, Hirono N, Hashimoto M, et al. Cognitive loss in dementia with Lewy bodies and Alzheimer's disease. Arch Neurol 1998; 55: 1547–52.

Spillantini MG, Crowther RA, Jakes R, Cairns NJ, Lantos PL, Goedert M. Filamentous alpha-synuclein inclusions link multiple system atrophy with Parkinson's disease and dementia with Lewy bodies. Neurosci Lett 1998; 251: 205–8.

Spinnler H, Tognoni P. Standardizzazione e taratura italiana di test neuropsicologici. Ital J Neurol Sci 1987; Suppl 6: 44–6.

Studholme C, Hill DL, Hawkes DJ. Automated three-dimensional registration of magnetic resonance and positron emission tomography brain images by multiresolution optimization of voxel similarity measures. Med Phys 1996; 24: 25–53.

Warrington EK, James M. The visual object and space perception battery test. Bury St Edmunds: Thames Valley Test Company; 1991.

Werring DJ, Clark CA, Barker GJ, Thompson AJ, Miller DH. Diffusion tensor imaging of lesions and normal-appearing white matter in multiple sclerosis. Neurology 1999; 52: 1626–32.